Jílek, M., Kulich, M., and Přeučil, L. (2020). **Centimeter-scaled Self-Assembly: A Preliminary Study**. In O. Gusikhin, K. Madani, & J. Zaytoon (Eds.), Proceedings of the 17th International Conference on Informatics in Control, Automation and Robotics (pp. 438–445). ScitePress https://doi.org/10.5220/0009830104380445.

Centimeter-scaled Self-assembly: A Preliminary Study

Martin Jílek, Miroslav Kulich and Libor Přeučil

Czech Institute of Informatics, Robotics, and Cybernetics, Czech Technical University in Prague, Czech Republic
{*Martin.Jilek.2, Miroslav.Kulich, Libor.Preucil*}*@cvut.cz*

Keywords: Passive self-assembly systems, robot swarms, multi-robot systems, smart materials, tile assembly.

Abstract: Passive self-assembly represents a general kind of bottom-up assembly process for objects, where the assembling particles exhibit no explicit, active "sense and affect" featuring, but embedded properties only. Although the majority of the previous work in the field has been performed on a microscopic scale, in the field of chemistry and nanotechnology, we identify a strong relation to macroscopic cases and principles studied in robotics. We show that passive self-assembly processes might be promising also towards the development of new, completely passive (multi)robot systems, driven entirely by environmental perturbations. This work sketches insight into fundamental principles of driving a centimeter-scale self-assembly system while observing the behavior of single particles. Investigations show, that not all the principles previously studied in the microscopic scale do hold also in the macroscopic cases of centimeter-scale particles. Thus, this article proposes the macroscopic problem specification and an experimental self-assembly system design consisting of entirely passive elements. We tackle a theoretical description of the system model and the necessary simplification towards a two-handed tile assembly model (2HAM) together with real-world experimentation design. We evaluate experimental results, discuss the feasibility of shake-driven macroscopic self-assembly, and elaborate their major properties together with estimated future work.

1 INTRODUCTION

Self-assembly is a natural behavior of many systems in our universe, from ensembles of elementary particles through biological systems to astronomical objects (Whitesides and Grzybowski, 2002) – yet it is not utilized much past the nanometer scale. This is probably going to change in future years when we master the potential hidden in this technology. The main principle of self-assembly, minimization of the potential energy of the assembling system, makes it very general and applicable at all scales, as long as it is physically feasible to produce individual components of the system which will assemble into larger parts.

Research of self-assembly was pioneered in the area of biology at the end of 20th century. Since the beginning, self-assembling elements are often made of DNA (like in (Winfree, 1998), (Chen and Seeman, 1991), (Jiang et al., 2017)). This, together with a mathematical understanding of the process, led to the design of systems where the result of the assembly can be precisely controlled. These shapes range from DNA assembly of Sierpinski triangle (Rothemund et al., 2004) to an assembly of complex 2D and 3D shapes using a technique called DNA origami (Rothemund, 2006), (Douglas et al., 2009). Nowadays, self-assembly is not only limited to DNA. For example, colloidal self-assembly of spherical polystyrene particles can be used on the micrometer scale (McGorty et al., 2010), (van Dommelen et al., 2018). Microscale also permits usage of capillary forces (like in (Hosokawa et al., 1996)), which even caused folding of macroscale objects (Wei et al., 2016) and self-assembly of tiles in a size of millimeters (Rothemund, 2000). Unlike most common manufacturing methods, self-assembly offers high positioning accuracy, it also scales very well with the number of assemblies we need to build because of its parallel nature (Boncheva and Whitesides, 2005).

1.1 Motivation

We explore the possibility of utilization of (at least a part of) knowledge from the area of tile-based self-assembly, as known in nanotechnology, in the centimeter-scaled world of robotics. Our idea is a construction of a universal assembling machine – a machine assembling arbitrary structures based on stochastic excitation of individual parts, which are en-

tirely passive. The target structure is encoded into the structure of individual parts at the beginning of the experiment and all the parts are being excited until they form the target pattern.

Our long term practical goal is the utilization of tile-based self-assembly methods in the manufacturing of objects made from modular metamaterials, like in (Nežerka et al., 2018). Such emerging materials posses interesting physical properties (like negative Poisson ration) and because their manufacturing requires precise placement of a large quantity of geometrically similar modules, we see this as an important application of tile-based self-assembly methods.

1.2 Related work

We are interested in the physical implementation of simple models of tile-based self-assembly, like the abstract tile assembly model (aTAM) which is already underlaid by a heavy body of theory. Such implementations were already shown in chemistry and nanotechnology as successful, nevertheless, in the centimeter-scaled world there is not much literature about the topic and most of it reports only assembly of simple shapes, like in (Masumori and Tanaka, 2013), (Daiko Tsutsumi and Satoshi Murata, 2007), (Egri and Bihari, 2018) or (Löthman, 2018).

Such passive self-assembly approaches can be divided into two groups (Cademartiri and Bishop, 2015): puzzle-based and strand-based.

The puzzle-based approach operates with freely moving tiles, which can bind together and form bigger assemblies. This approach originated from biology ((Winfree, 1998), (Chen and Seeman, 1991), (Jiang et al., 2017), (Rothemund et al., 2004), (Rothemund, 2006), (Douglas et al., 2009)). Here, elementary building tiles are constructed using DNA. Most implementations use rectangular tiles, where each side has some kind of binding site. The type of the site ensures reactivity just with the matching sites of other tiles. This passive branch of self-assembly is backed by mathematical models and guarantees on assembly feasibilities and complexities. One of the most theoretically explored models is the abstract tile assembly model (aTAM), which models the tile system as a set of massless non-rotating tiles, binding themselves to seed according to their binding site parameters and a system-wide temperature parameter (Winfree, 1998). Possible generalization of aTAM is a 2HAM model (Patitz, 2014), which removes the need for seed and enables interaction of all assemblies in parallel.

The strand-based approach is inspired by protein folding. Tiles are the same as in the puzzle-based assembly but are also connected to the 1D chain. This can lower the number of encoded specific interactions in the system but poses another difficulty during the design of flexible interconnections of tiles in the chain (Cademartiri and Bishop, 2015). It was proven that it is possible to fill any continuous area or volumetric shape with such a technique (Cheung et al., 2011).

Such passive systems have several plausible properties. They can be manufactured cheaply, which permits large scale experiments. They are an interesting addition to manufacturing technology, offering a possibility to assemble 3D parts too small for conventional manufacturing. (Boncheva and Whitesides, 2005) They also mimics fundamental processes on which our world is built upon. Research of the behavior of such a system can result in knowledge transferable to other scientific areas like biology. (Boncheva et al., 2003)

1.3 Contributions

The main contribution of this article is the development of a prototype of a passive robotic swarm platform exhibiting self-assembly behavior. The system resembles the theoretical models of the tile-based self-assembly. It consists of a set of independent (and completely passive) tiles and a reactor, in which the assembly takes place.

We tested the system on two assembly scenarios resembling the sHAM model, which we derived from the commonly used 2HAM model. The results lead us to the conclusion that the assembly of at least simple structures is possible in a reasonable time.

1.4 Content of the Article

The article is structured as follows. In Section 2 we described individual steps in the design of the self-assembly system. Firstly, we propose a simplified model of the tile-based self-assembly system, derived from the 2HAM model. Secondly, the mechanical design of the system is described along with a theoretical model of tile-tile interaction. In the third part, we describe the reactor used to supply kinetic energy to the system during experiments. The last part describes the visual tracking system. Section 3 qualitatively evaluates the behavior of our prototype. All the results are summarized in section 4.

2 METHODOLOGY

Our research question can be formulated as follows: *is it possible to create a centimeter-scale pas-*

sive robotic system exhibiting a self-assembly behavior, as described by the 2HAM model?

Informally, tile-based self-assembly assumes that the assembling system consists of a set of tiles (Fig. 1), moving freely in a reactor (either in 2D or 3D). Sides of the tiles contain binding sites, which can cause that two tiles stick together upon contact. The binding sites can be of different types, which restricts the bonding interactions between the tiles, and, as a result, the assembly will result in different objects. Many mathematical models of such a process exist, as in (Patitz, 2014). We derived our own assembly model (based on assumptions closer to the physical reality) in the first part of the work. The physical prototype was designed in a way that resembles the model as much as possible. We also proposed a solution to the problem of finding sets of suitable encodings of tile-tile interactions. Constructed prototype was placed into the reactor (section 2.4) equipped with visual tracking system (section 2.5) and several experiments were performed.

2.1 Formal Self-assembly Model

Our tile design is inspired by a group of often mentioned tile assembly models, namely abstract tile assembly model (aTAM) (Winfree, 2006), kinetic tile assembly model (kTAM) (Winfree, 2006) and, especially, two-handed assembly model (2HAM) (Patitz, 2014). These models have some limiting restrictions, but are often mentioned in literature and a large corpus of a theory is dedicated to them.

Informally, the 2HAM model represent tiles as non-rotating objects with 4 sides (see Fig. 1a), placed on integer-valued lattice, which can bind to other (matching) sides or assemblies iff the resulting bond will be strong enough (as in Fig. 1b). Nevertheless, the 2HAM model forbids rotation of the tiles and assumes an infinite number of tiles (which is not our case). Thus, we present a relaxed variant, the *simplified two-handed assembly model*:

Definition 2.1 (sHAM)**.** *Simplified two-handed assembly model (sHAM) is a tuple* (T,S,I,τ)*, where T is a set of tile types, S is an initial state, I is a glue strength function and* $\tau \in \mathbb{N}$ *is a system temperature.*

Definition 2.2 (Tile type)**.** *Tile type t is a 5-tuple of a label l and four glues* $(l,\sigma_N,\sigma_E,\sigma_S,\sigma_W)$*, where* $\sigma \in \Sigma$*. Each glue is associated with one direction from* $\{(0,1),(-1,0),(0,-1),(1,0)\}$.

Definition 2.3 (Tile instance)**.** *Each tile instance is a tuple* (t,p)*, where p is a position of a tile in an integer-valued unit 2D orthogonal lattice. Tile type t of a particular tile instance can change during the experiment because of a* ***rotation*** *- glue assignment in t will shift to the left or to the right. The position p can change because of a* ***movement*** *of a tile instance. Each position in the sHAM lattice can be occupied by at most one tile instance.*

Definition 2.4 (Initial state)**.** *The initial state S is a multiset of tile instances.*

Definition 2.5 (Interaction of glues)**.** *Two tile instances* a,b *are in neighborhood iff their distance is equal to one. Glues* g_a,g_b *of* a,b *can interact iff* a,b *are in neighborhood and iff for direction vectors* $\vec{d_a}$ *and* $\vec{d_b}$*, associated with* g_a,g_b*, holds* $\vec{d_a} = -\vec{d_b}$*. Let all such pairs of glues be called interacting glues of a,b.*

Definition 2.6 (Interaction strength)**.** *Interaction is ruled by* $I : \Sigma \times \Sigma \to \mathbb{Z}$*, where* Σ *is the set of glue types (arbitrary symbols, we restricted ourselves to integers). Two tiles (or assemblies) can form a stable assembly iff the sum of strengths of all their interacting glues is at least equal to* τ*.*

An example of one such tile and a whole assembly is shown in Fig. 1.

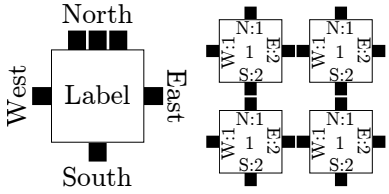

(a) Abstract model of a tile (b) Example of an assembly

Figure 1: Model of a tile (1a) and example of a valid assembly. Each instance of tile type carry 4 glues on its side. The tiles form bigger assemblies on an orthogonal 2D lattice whenever matching glues (1,2) meet together and their combined strength is higher than external disturbances (1b).

2.2 Design of a Tile

Tile design significantly contributes to the success of the assembly. All tiles are geometrically the same and roughly follow the 4-sided rectangular shape of the tile of our idealized model (Figure 1a). The implementation of the bonding mechanism is purely magnetic. Each side of the tile has three channels for replaceable magnet holders. The configuration of magnets on each side of each tile determines the behavior of the system.

Since our physical realization encodes the interactions into 2D arrangements of magnets, it could happen that two such binding sites stick together only partially, which leads to an invalid assembly. Thus,

the sides of our experimental tiles are curved to prevent horizontal misalignment. The shape is inspired by (Haghighat et al., 2015), but is more curved, which makes the potential energy landscape of the system smoother. Thus it contains less local minima which can trap the evolution of the system in an undesired state. Moreover, to prevent vertical shifts of magnetic codes, the tile is also equipped with vertical locks.

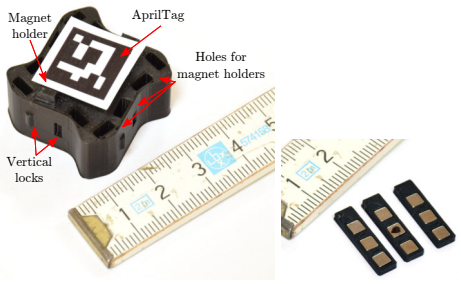

(a) (b)

Figure 2: The physical realization of a tile (left) and a complete set of magnet holders that encode bond on one side of the tile.

The width of the tile is 3 cm, height 1.5 cm. Weight is 6.28 g. Tiles were printed from PLA plastics on a Prusa MK3S printer with a 0.4 mm extruder. No infill was used to make them as light as possible for possible future experiments in a liquid environment. The printing of one tile without magnet holders takes 54 minutes. AprilTag (Krogius et al., 2019) fiducial marker is glued on top of each tile for automatic evaluation of experiments via a vision-based system.

2.3 Encoding of Interactions Between Tiles

Each side of each tile carries code assembled from permanent magnets. The magnets are assembled into a 3×3 matrix with various orientation of south and north poles. Formally:

Definition 2.7 (Glue plate)**.** *Glue plate A is a matrix of size $m \times n$. Glue plate contains numbers from the set $\{-1, 0, 1\}$, where -1 is a magnetic south pole, 1 a north pole and 0 no magnet.*

Let us propose the *(abstract) magnetic interaction model*, which assumes that magnets on glue plates interact only when the tiles touch together and neglects the effect of magnetic crosstalk:

Definition 2.8 (Magnetic interaction model)**.** *Let H^{AB} be a matrix formed as a Hadamard product of two glue plates A, B with dimensions $m \times n$:*

$$H^{AB} = A \odot B \tag{1}$$

Interaction strength between interacting (neighboring) glue plates A and B is then:

$$F(A,B) = -\sum_{r=0}^{m}\sum_{c=0}^{n} H^{AB}_{cr} \tag{2}$$

Interaction between non-interacting (non-neighboring) plates is 0.

Thus, for the practical implementation of a tile assembly model, we need to determine all the glue plates in the system. In simple cases (where only a small number of glue plates is needed) they can be designed manually. For complex cases, the task can be formulated as a constraint satisfaction problem, where we search for the set of glue plates satisfying constraints given by the Definition 2.8.

Magnetic plates were realized with the use of NdFeB magnets (N50) with a size $3 \times 3 \times 1$ mm. The magnets are arranged into bars of size $18 \times 5 \times 1.6$ mm. Each such bar can support 3 magnets. An example of 3 such bars, ready to be placed into the holder on one side of a tile, can be seen in Figure 2b. Each magnet bar, printed from PLA with a 0.4 mm extruder, weights 0.14 g. The printing time of each is 2.5 minutes.

2.4 Design of the Reactor

The purpose of the reactor (Fig. 3) is to supply mechanical energy to the system and to achieve a sufficiently random movement of tiles. For our initial experiments, we constructed a circular cardboard reactor (with a diameter of 30 cm), which is mounted on a 6DoF robotic manipulator (UR5) to provide excitation energy. The reactor is also equipped with a camera, observing the process from the top (such that the optical axis is perpendicular to the plane on which the tiles move).

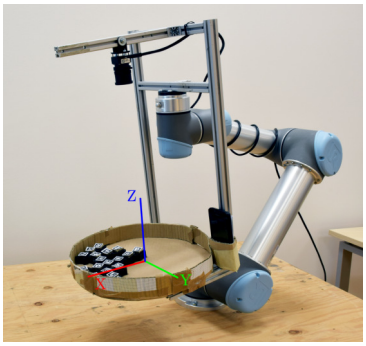

Figure 3: The reactor mounted on a robotic manipulator. The reactor coordinate frame, used through this work, is marked.

2.5 Visual Tracking of a Self-assembly Process

A possibility of observation of the self-assembly on the scale of individual tiles in real-time is one of the reasons why macroscopic self-assembly could bring insight into similar processes on a smaller scale. It could be also used for fine-grained feedback control of the reactor.

Our setup assumes that the motion of each tile is planar and that the excitation energy is provided by the movement of the whole reactor. Because of that, the camera was fixed to the reactor above the plane of motion of tiles such that its optical axis is perpendicular to the plane. This solution keeps all the tiles in the focal plane. The first step of the visual

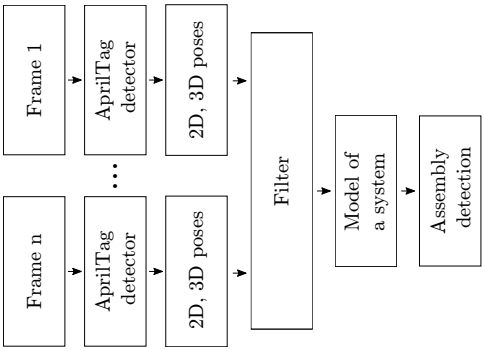

Figure 4: Visual tracking pipeline.

tracking pipeline (Fig. 4) is the detection of AprilTags (with the usage of apriltags3-py library) on each frame from the camera. It outputs poses of tiles in 3D and also in image coordinates. The filtering stage then linearly interpolates missing values (where the detector failed to identify the tag) and the kinematic model of the system is finally used to perform assembly detection. The kinematic model of a system is similar to the abstract model (Definition 2.1). Each tile instance is modeled as a matrix T, where s is the width of the tile. Each column d_l represents the position of one glue w.r.t. the local coordinate frame of the tile:

$$T = \begin{bmatrix} 0 & \frac{-s}{2} & 0 & \frac{s}{2} \\ \frac{s}{2} & 0 & \frac{-s}{2} & 0 \end{bmatrix} \tag{3}$$

The tracking system determines tile translation $\vec{t}$ and rotation R. Let positions of glues of tiles 1 and 2 in the camera reference frame be

$$\begin{aligned} T_{1c} &= RT_1 + \vec{t_1} \\ T_{2c} &= RT_2 + \vec{t_2} \end{aligned} \tag{4}$$

The bond between tiles $1,2$ is detected only between glues with position vectors (w.r.t. camera frame) $\vec{d}_{c1}, \vec{d}_{c2}$ which satisfy the following conditions:

$$\begin{aligned} |\vec{d}_{c1} - \vec{d}_{c2}| &< \varepsilon_{trans} \\ (\vec{d}_{c1} - \vec{t}_1) \cdot (\vec{d}_{c2} - \vec{t}_2) &< \varepsilon_{rot} \end{aligned} \tag{5}$$

where $\varepsilon_{trans}, \varepsilon_{rot}$ are predefined thresholds. Moreover, the detector also permits detection of bonds using the same criteria, but in image coordinates (which can be beneficial with noisy observations).

This procedure outputs one *bonding graph* $G_B = (V,E)$ for each frame, where V is a set of tile instances and E is a set of edges formed between pairs of tiles with stable bonds. All edges in G_B must satisfy conditions (1) and (2). Complex assemblies are then found as connected components of G_B.

3 RESULTS

We designed two experiments to test the system. In both scenarios, a set of 20 tiles was placed into the reactor, which performed back-and-forth movement along the reactor x-axis with small swings around y-axis. The amplitude of linear acceleration along the x-axis was chosen as a parameter related to the system temperature. It was experimentally set to the lowest value where the individual tiles overcome the friction forces and start moving (almost) independently of the reactor (see Fig. 5). The amplitude of the position change (Fig. 6) during movement was fixed at a value where the tiles start to collide with opposing walls of the reactor. The reactor was slightly rotated around its x-axis during the whole motion to keep the tiles in one cluster to maximize the probability of collisions.

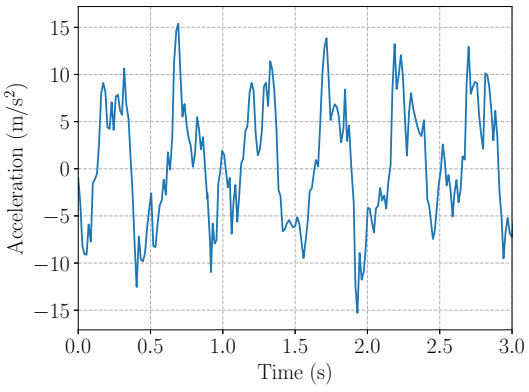

Figure 5: Acceleration of the reactor measured in prevailing (x) axis of movement.

Glues used in both experiments were of type G_0,

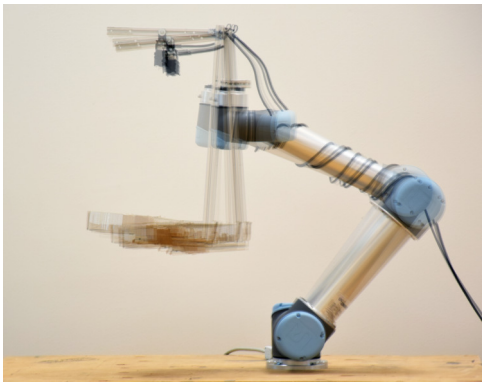

Figure 6: Motion of a manipulator.

G_1 and G_2. In a formalism of the Definition 2.8:

$$G_0 = \begin{bmatrix} 0 & 0 & 0 \\ 0 & 0 & 0 \\ 0 & 0 & 0 \end{bmatrix} \quad G_1 = \begin{bmatrix} 0 & 0 & 0 \\ 0 & 1 & 0 \\ 0 & 0 & 0 \end{bmatrix} \quad G_2 = \begin{bmatrix} 0 & 0 & 0 \\ 0 & -1 & 0 \\ 0 & 0 & 0 \end{bmatrix} \tag{6}$$

Both experiments were repeated with different random initial placement of tiles and evaluated by the visual tracking system incorporated into the assembly reactor.

3.1 Self-assembly of Boxes

In this experiment, we aimed for an assembly of boxes composed of 2×2 tiles. Our system consisted of one tile type (Fig. 7a), with two types of glues, which permits four assemblies to be present during the assembly process (Fig. 7b).

(a) (b)

Figure 7: Tile model and a set of possible products (A, B, C, D) for the box assembly experiment.

The experiment was ended when the number of completed boxes stabilized for a sufficiently long time. Equidistantly sampled images of the process are visible in Figure 8. Results of automatic analysis of the whole experiment are shown in Fig. 9 and Fig. 10.

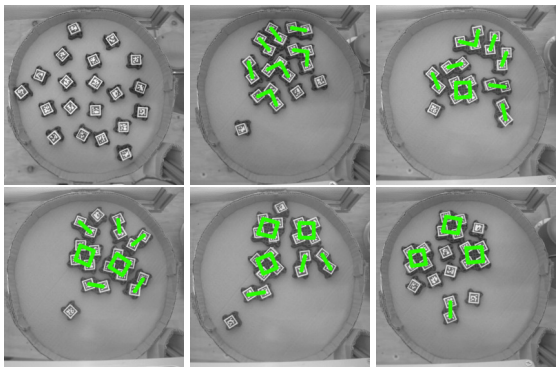

Figure 8: Attempt to self-assemble 2×2 boxes. The images (from left to right, top to bottom) were captured in approx. 24-second intervals.

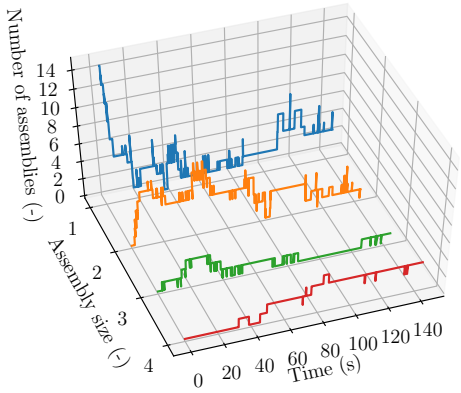

Figure 9: Number of assemblies of all possible sizes during the assembly of boxes in the experiment depicted in Fig. 8.

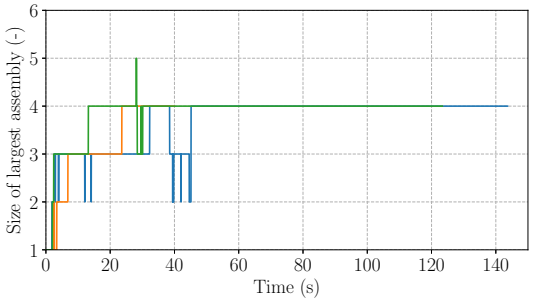

Figure 10: Size of the largest assembly present at each timestamp during three runs of the assembly of boxes. The spike at 30 s is an artifact caused by the visual tracking system.

3.2 Self-assembly of Linear Chains

This experiment explores the behavior of a tilesystem which is designed to form linear segments of unlimited length. Tiles were designed according to the Figure 11a. Evaluation of assembly progress resulted in figures 13 and 14.

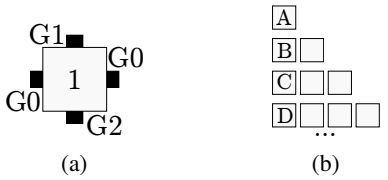

(a) (b)

Figure 11: Tile model (a) and a set of possible linear assemblies (A, B, C, D, ...) for the chain assembly experiment (b).

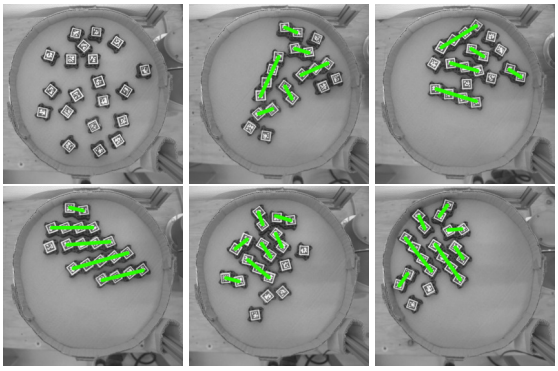

Figure 12: Attempt to self-assemble linear segments of unlimited length. The images (from left to right, top to bottom) were captured in approx. 19-second intervals.

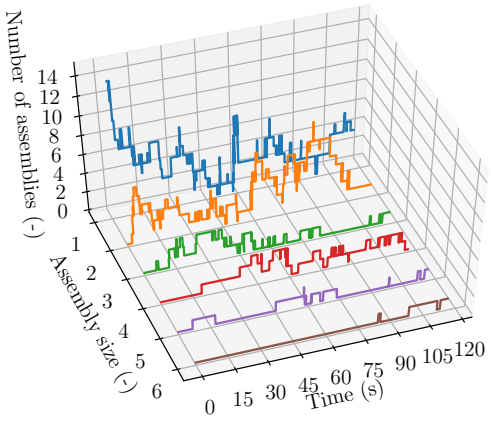

Figure 13: Number of assemblies of all possible sizes during the assembly of linear chains as in Fig. 12.

3.3 Observations

The following facts are visible from both types of experiments and captured data:

- **Single tiles** are highly reactive, after the start of the experiment almost all of them are incorporated into dimers in a few seconds.
- **L-shaped trimers** appear after the concentration of dimers exceeds a certain limit. Nevertheless, they are not stable and quickly form tetramers or dissolve into dimers and monomers.

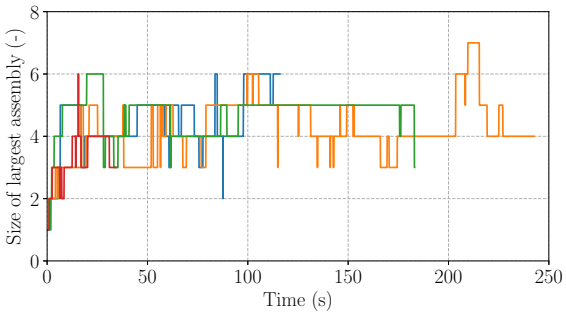

Figure 14: Size of the largest assembly present at each timestamp during four runs of the assembly of linear chains.

- **Box-shaped tetramers** are extremely stable. They exhibit a kind of self-repairing behavior. Their destruction often results in two dimers, which again form the same tetramer in a matter of seconds.
- **Longer chains** tend to form clusters, where all assemblies are parallel. This leads to a higher stability and self-repair behavior because chains in these clusters have a degree of structural flexibility.
- Both experiments ended up in **equilibrium**, which was similar for different trials of the same experiment.

4 CONCLUSIONS

This paper presents a novel macroscopic robotic system capable of tile-based 2D self-assembly together with preliminary experiments. The system is composed of entirely passive elements – tiles – whose interactions are fixed before the start of the assembly. The whole system is continuously excited by uncontrolled mechanical disturbances from the environment and the formation of patterns (pre-programmed into interactions between tiles) is observable as the potential energy of the system decreases.

Our experimental results suggest that the programmable tile-based assembly is feasible in the centimeter-scaled world. Unlike our expectations, the macroscopic self-assembly of simple shapes is fast (assembly times of structures containing 4-6 tiles are in order of tens of seconds) and assemblies are stable on time intervals of seconds for unstable shapes to tens of seconds for stable shapes.

Future work should be focused on multiple areas: (1) Assembly of more complex shapes within the framework of aTAM and kTAM models, (2) real-time control of the external disturbance to optimize assembly times, (3) improvement of the tracking system,

which in the current state requires manual preparation (search for optimal detection thresholds, precise lightning of the experiment) when used with a noisy or low-resolution camera. (4) The evolution of the system should be also studied over a longer time-scale since some experiments (like in Figure 12) suggest the presence of cyclic behavior. (5) Future work should also focus on the quantitative analysis of the process in the context of the proposed model.

ACKNOWLEDGEMENTS

The research leading to these results has received funding from the Czech Science Foundation (GAČR) under grant agreement no. 19-26143X. The work of Miroslav Kulich has been supported by the European Regional Development Fund under the project Robotics for Industry 4.0 (reg. no. CZ.02.1.01/0.0/0.0/15 003/0000470).

REFERENCES

Boncheva, M., Bruzewicz, D., and Whitesides, G. (2003). Millimeter-scale self-assembly and its applications. *Pure Appl. Chem*, 75:621–630.

Boncheva, M. and Whitesides, G. (2005). Making things by self-assembly. *MRS Bulletin*, 30:736–742.

Cademartiri, L. and Bishop, K. J. M. (2015). Programmable self-assembly. *Nature materials*, 14 1:2–9.

Chen, J. and Seeman, N. C. (1991). Synthesis from DNA of a molecule with the connectivity of a cube. *Nature*, 350:631–633.

Cheung, K. C., Demaine, E. D., Bachrach, J. R., and Griffith, S. (2011). Programmable assembly with universally foldable strings (moteins). *IEEE Transactions on Robotics*, 27(4):718–729.

Daiko Tsutsumi and Satoshi Murata (2007). Multistate part for mesoscale self-assembly. In *SICE Annual Conference 2007*, pages 890–895.

Douglas, S. M., Dietz, H., Liedl, T., Hogberg, B., Graf, F., and Shih, W. M. (2009). Self-assembly of DNA into nanoscale three-dimensional shapes. In *Nature*.

Egri, S. and Bihari, G. (2018). Self-assembly of magnetic spheres: a new experimental method and related theory. *Journal of Physics Communications*, 2.

Haghighat, B., Droz, E., and Martinoli, A. (2015). Lily: A miniature floating robotic platform for programmable stochastic self-assembly. In *2015 IEEE International Conference on Robotics and Automation (ICRA)*, pages 1941–1948.

Hosokawa, K., Shimoyama, I., and Miura, H. (1996). Two-dimensional micro-self-assembly using the surface tension of water. *Sensors and Actuators A: Physical*, 57(2):117 – 125. Ninth International Workshop on Micro Electro Mechanical System.

Jiang, S., Hong, F., Hu, H., Yan, H., and Liu, Y. (2017). Understanding the elementary steps in DNA tile-based self-assembly. *ACS Nano*, 11(9):9370–9381. PMID: 28813590.

Krogius, M., Haggenmiller, A., and Olson, E. (2019). Flexible layouts for fiducial tags. In *2019 IEEE/RSJ International Conference on Intelligent Robots and Systems (IROS)*, pages 1898–1903.

Löthman, P. A. (2018). *Macroscopic magnetic self-assembly*. PhD thesis, University of Twente, Netherlands.

Masumori, A. and Tanaka, H. (2013). Morphological computation on two dimensional self-assembly system. In *ACM SIGGRAPH 2013 Posters*, SIGGRAPH 13, New York, NY, USA. Association for Computing Machinery.

McGorty, R., Fung, J., Kaz, D., and Manoharan, V. N. (2010). Colloidal self-assembly at an interface. *Materials Today*, 13(6):34 – 42.

Nežerka, V., Somr, M., Janda, T., Vorel, J., Doškář, M., Antoš, J., Zeman, J., and Novák, J. (2018). A jigsaw puzzle metamaterial concept. *Composite Structures*, 202:1275–1279.

Patitz, M. J. (2014). An introduction to tile-based self-assembly and a survey of recent results. *Natural Computing*, 13(2):195–224.

Rothemund, P. W. K. (2000). Using lateral capillary forces to compute by self-assembly. *Proceedings of the National Academy of Sciences*, 97(3):984–989.

Rothemund, P. W. K. (2006). Folding DNA to create nanoscale shapes and patterns. *Nature*, 440:297–302.

Rothemund, P. W. K., Papadakis, N., and Winfree, E. (2004). Algorithmic self-assembly of DNA Sierpinski triangles. *PLoS Biology*, 2:1021 – 1024.

van Dommelen, R., Fanzio, P., and Sasso, L. (2018). Surface self-assembly of colloidal crystals for micro- and nano-patterning. *Advances in Colloid and Interface Science*, 251:97 – 114.

Wei, S., Qin, M., and Zhang, J. (2016). Mechanism and application of capillary-force self-assembly micro/nanofabrication. In *2016 IEEE International Conference on Manipulation, Manufacturing and Measurement on the Nanoscale (3M-NANO)*, pages 256–260.

Whitesides, G. M. and Grzybowski, B. A. (2002). Self-assembly at all scales. *Science*, 295:2418–2421. 793.

Winfree, E. (1998). *Algorithmic self-assembly of DNA*. PhD thesis, Caltech.

Winfree, E. (2006). Algorithmic self-assembly of DNA. In *2006 International Conference on Microtechnologies in Medicine and Biology*, page 4.